



Estimating the velocity and transport of Western Boundary Currents systems using Altimetry, XBT, and Argo: Case study of the East Australian Current



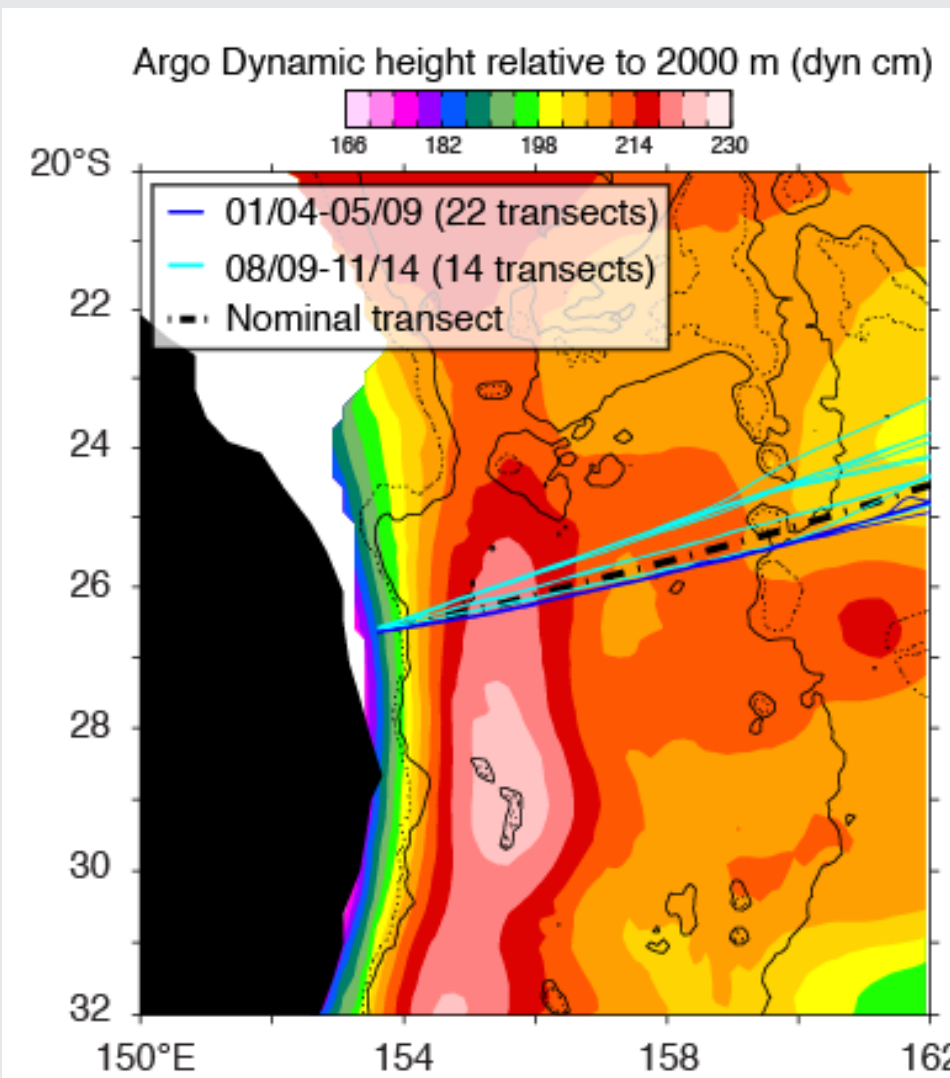
Nathalie Zilberman (nzilberman@ucsd.edu), Dean Roemmich, Sarah Gille
Scripps Institution of Oceanography, La Jolla California

Background

Calculating Western Boundary Current (WBC) transport is a challenging task. Fine resolution is necessary to resolve the narrow path of WBCs. Analysis regions should extend far enough offshore to depths greater than 1000 m. High-frequency sampling is needed to resolve the temporal variability of WBC systems. No single platform meets all criteria. For this reason, a preferred strategy is to combine multiple data sources.

Method

High-resolution XBT (HRX) PX30 (AUS/SIO)



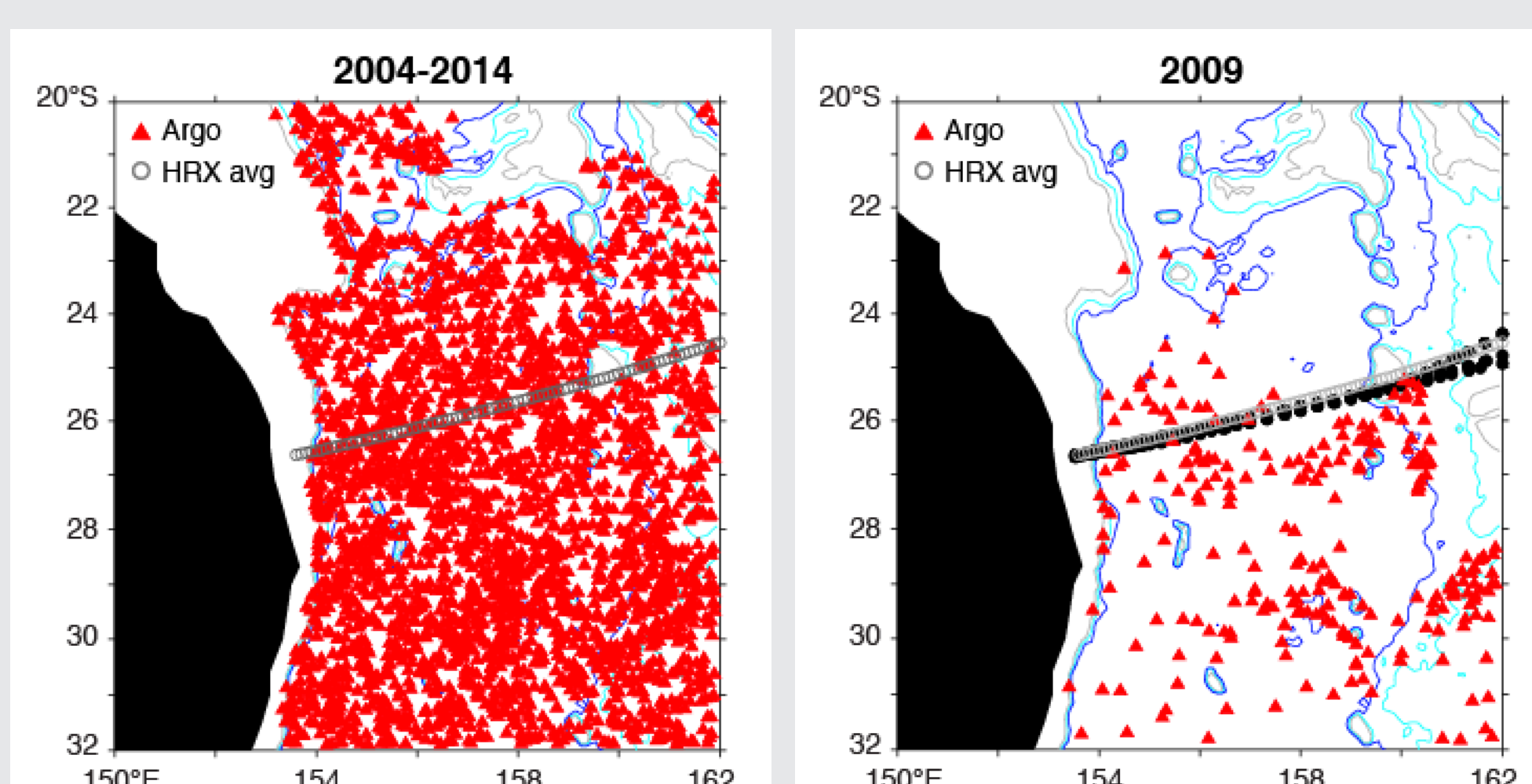
36 transects (2-4/yr) in 2004-2014 run across the EAC region.

Spatial transect sampling of 30-40 km along track decreasing to 10 km near boundaries.

Salinity inferred using Argo (T,S) curve.

Argo array

Range of 20-50 Argo floats per $1^\circ \times 1^\circ$ bin for 2004-2014. HRX transects obtain much denser coverage than Argo along selected lines. HRX sampling extends further shoreward than Argo (in shallow region and strong EAC shear).

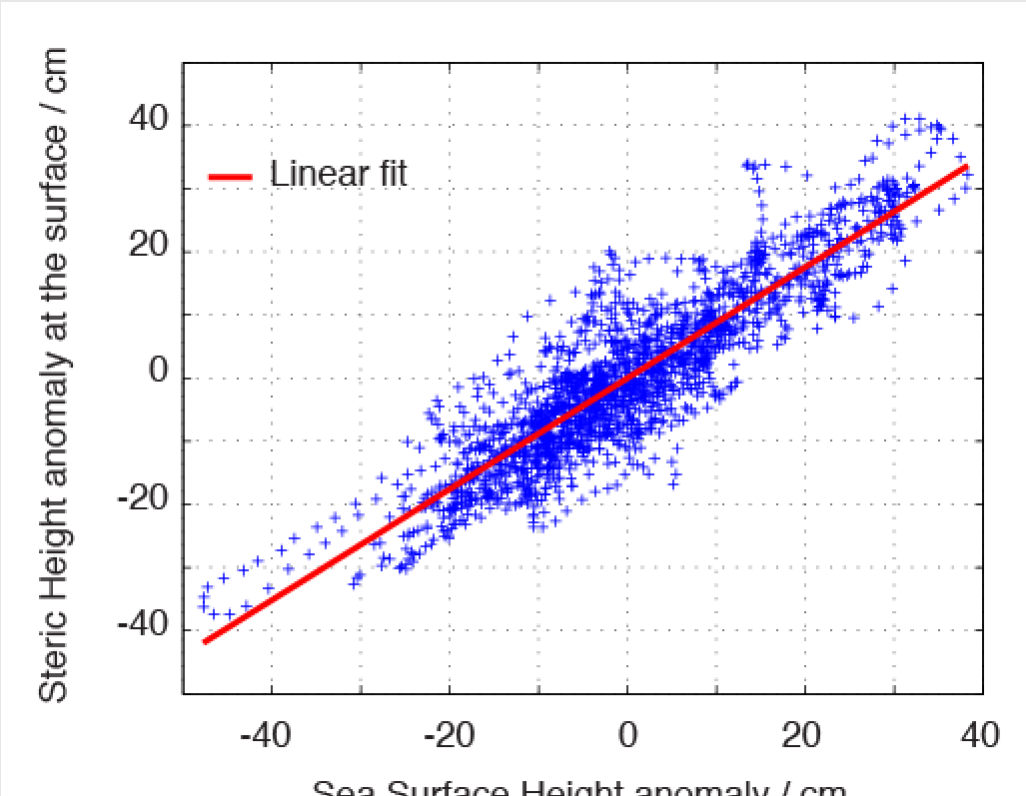


XBT temperature and salinity profiles along each track are projected onto a nominal transect using Argo maps of temperature and salinity.

XBT shear below 700 m depth is inferred using Argo-based correlation between dynamic height and temperature at 700 m depth at [24-29°S; 153-162°E] following Ridgway and Godfrey (1994 and 1997).

XBT absolute velocity is computed using Argo trajectory-based velocity at 1000 m depth.

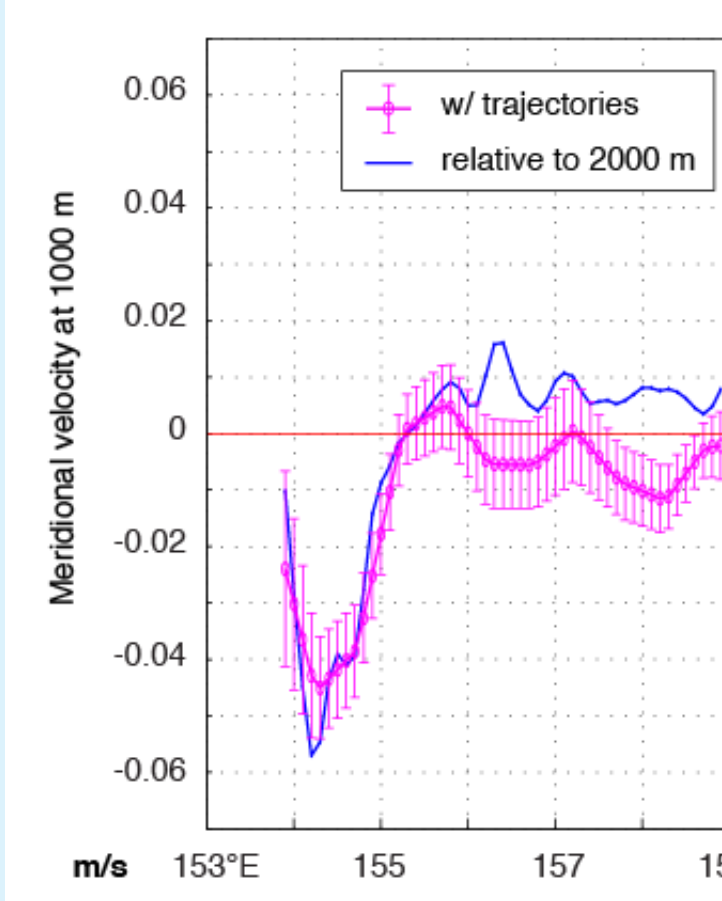
Altimetry



Sea surface height anomalies (AVISO, two-sat merged) in the EAC region are highly correlated with sub-surface temperature and salinity changes at inter-annual time scales.

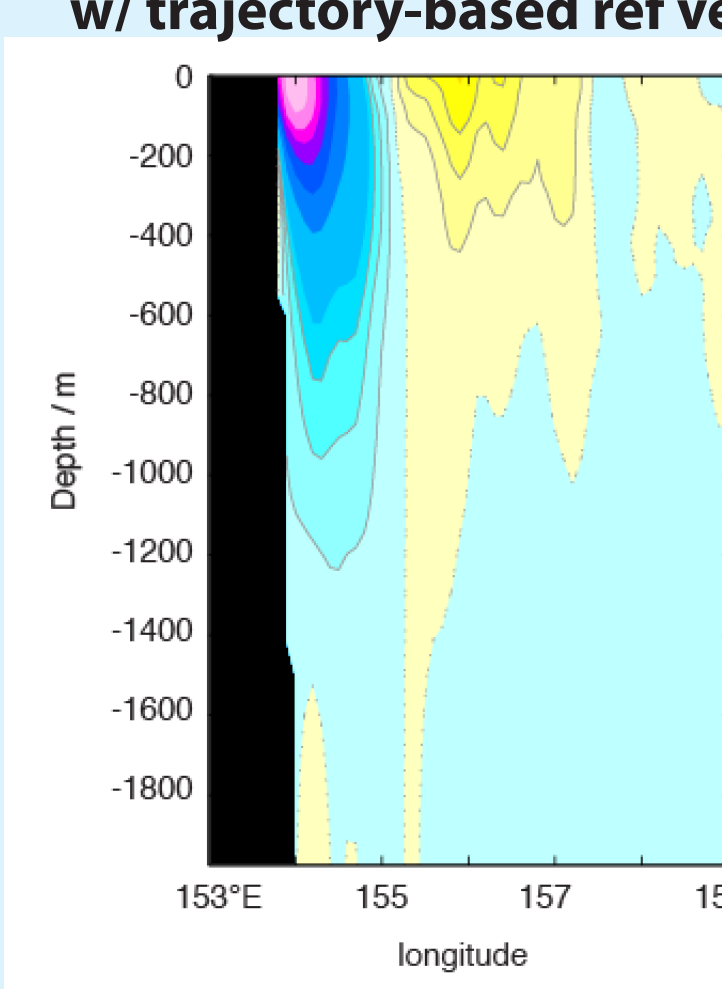
Linear regression coefficients are computed between sea surface height and XBT/Argo temperature and salinity time series to capture the signature of the highly variable eddy-like features in the vicinity of the EAC.

Mean geostrophic velocity in the EAC region

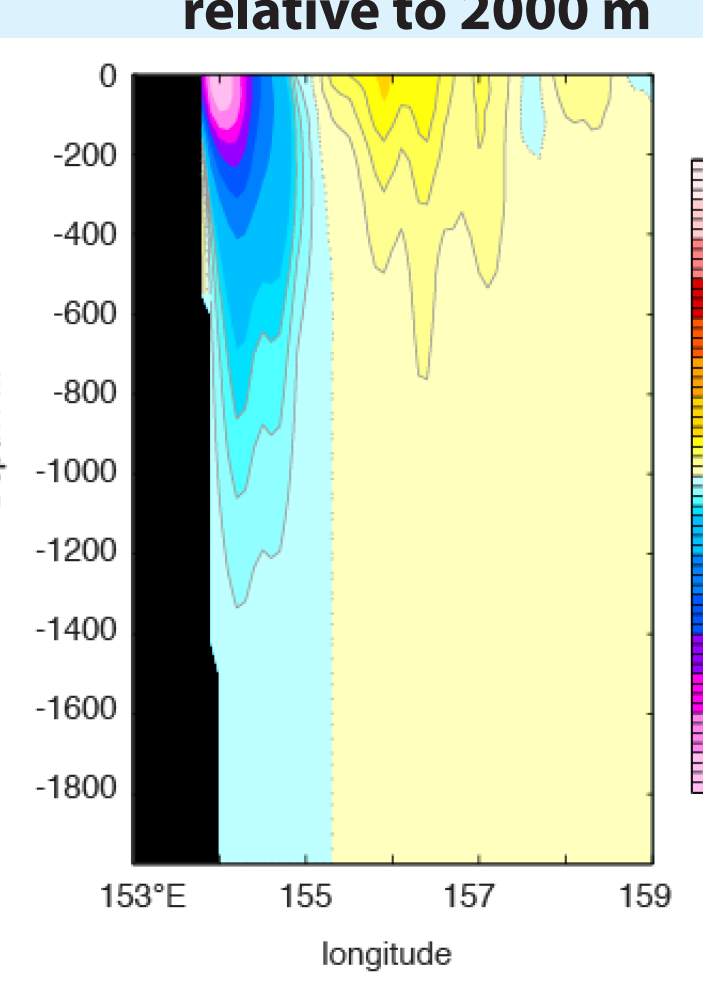


To preserve the sharp velocity gradients associated with the along-coast flow and flow reversal in the EAC region, trajectory-based velocities are sorted into $1/6^\circ$ latitude $\times 1/2^\circ$ longitude bins aligned with the 1000-m isobath. The $1/6^\circ$ latitude bins are then grouped into 3° latitude bins.

Absolute velocity using XBT/Argo w/ trajectory-based ref velocity



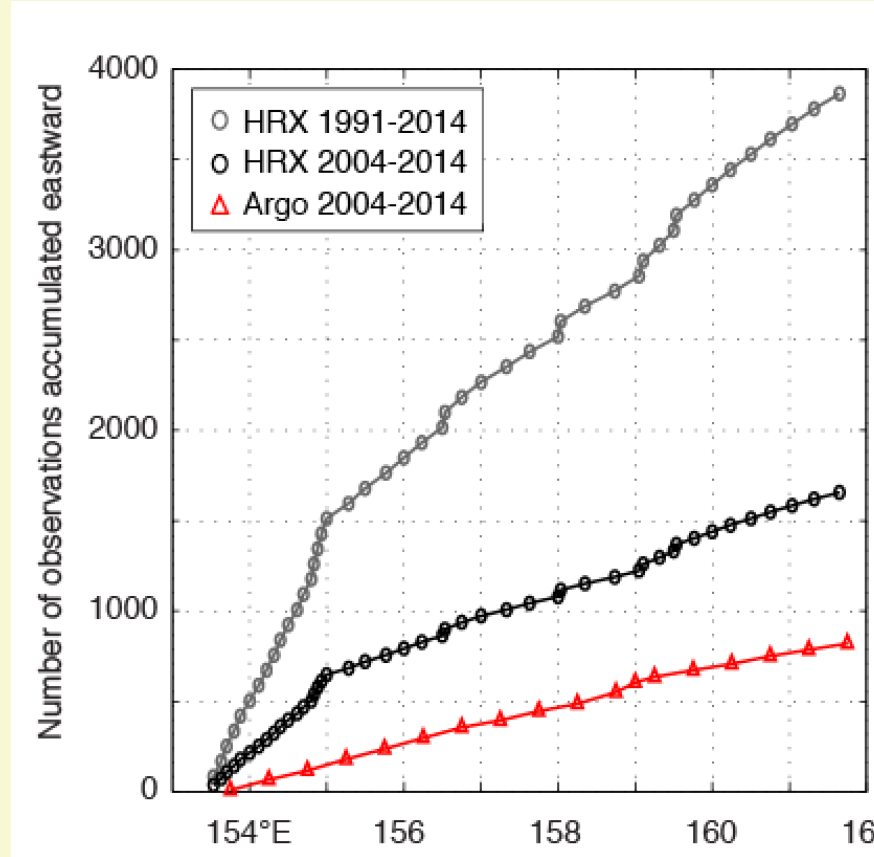
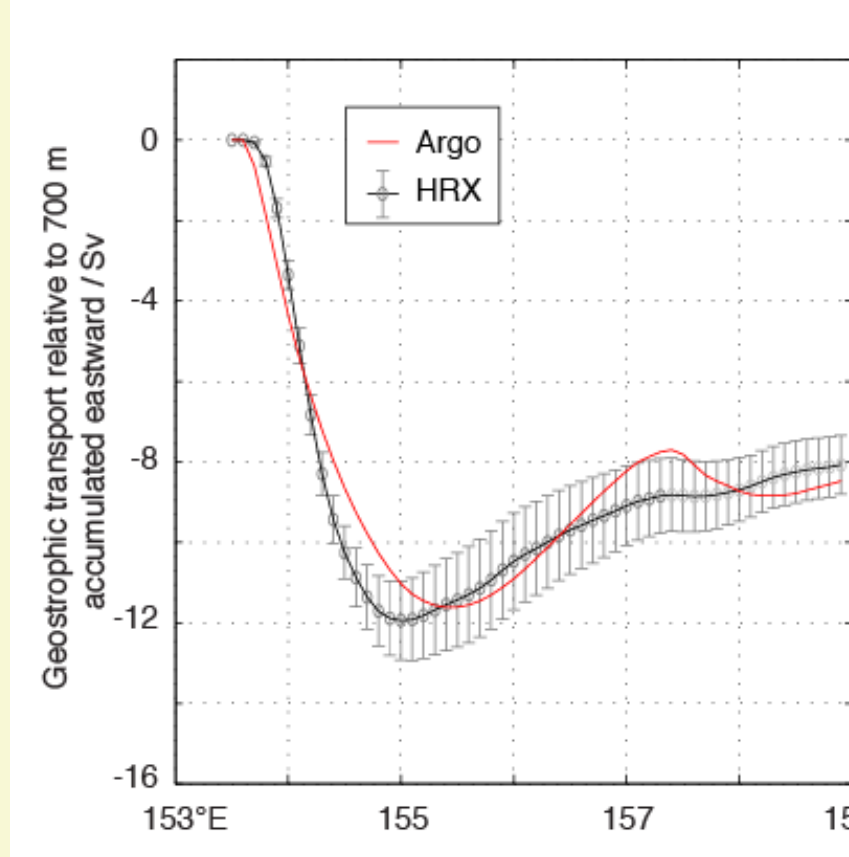
Velocity using XBT/Argo relative to 2000 m



Argo trajectories show less negative velocity than hybrid XBT/Argo velocity at 1000/2000 m. Trajectories "feel" the equatorward undercurrent observed by Mata et al. (2000).

Mean volume transport in the EAC region

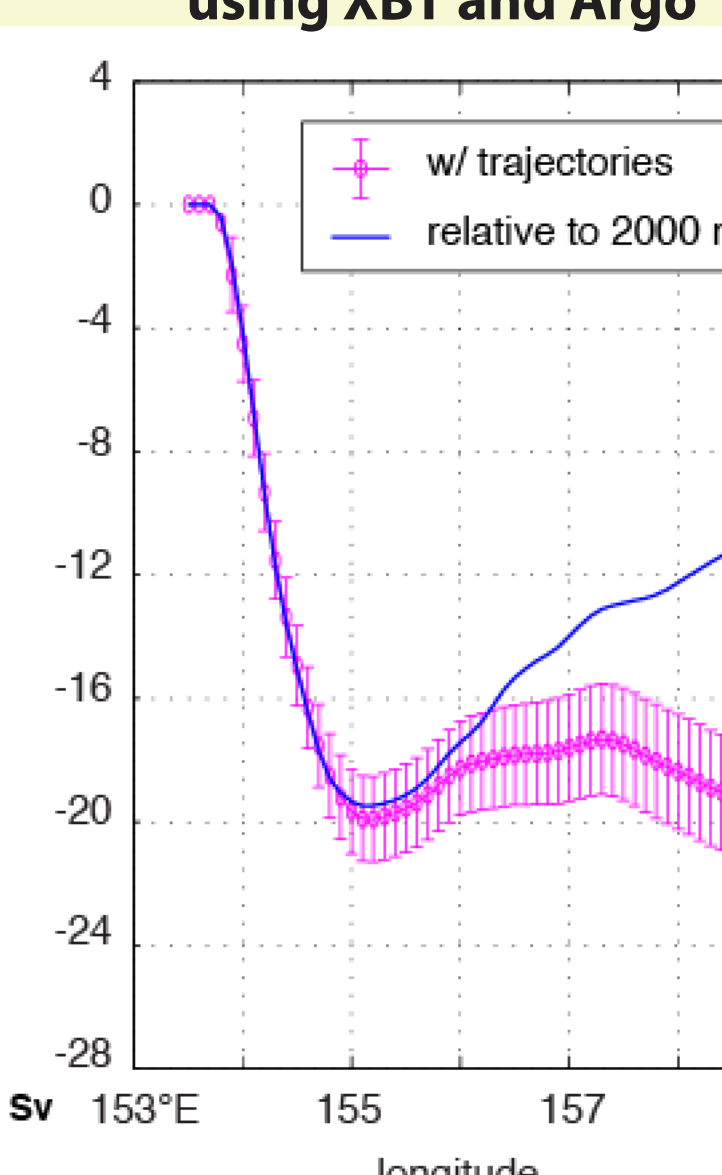
0-700 m



The 0-700 m EAC transport is 11.7 Sv using XBT and 11.4 Sv using Argo. For estimating geostrophic shear across the given track in the upper 700 m, HRX transects have less random error and sampling/coverage bias (from along-current averaging and near-shore data) than Argo.

0-2000 m

0-2000m geostrophic transport using XBT and Argo

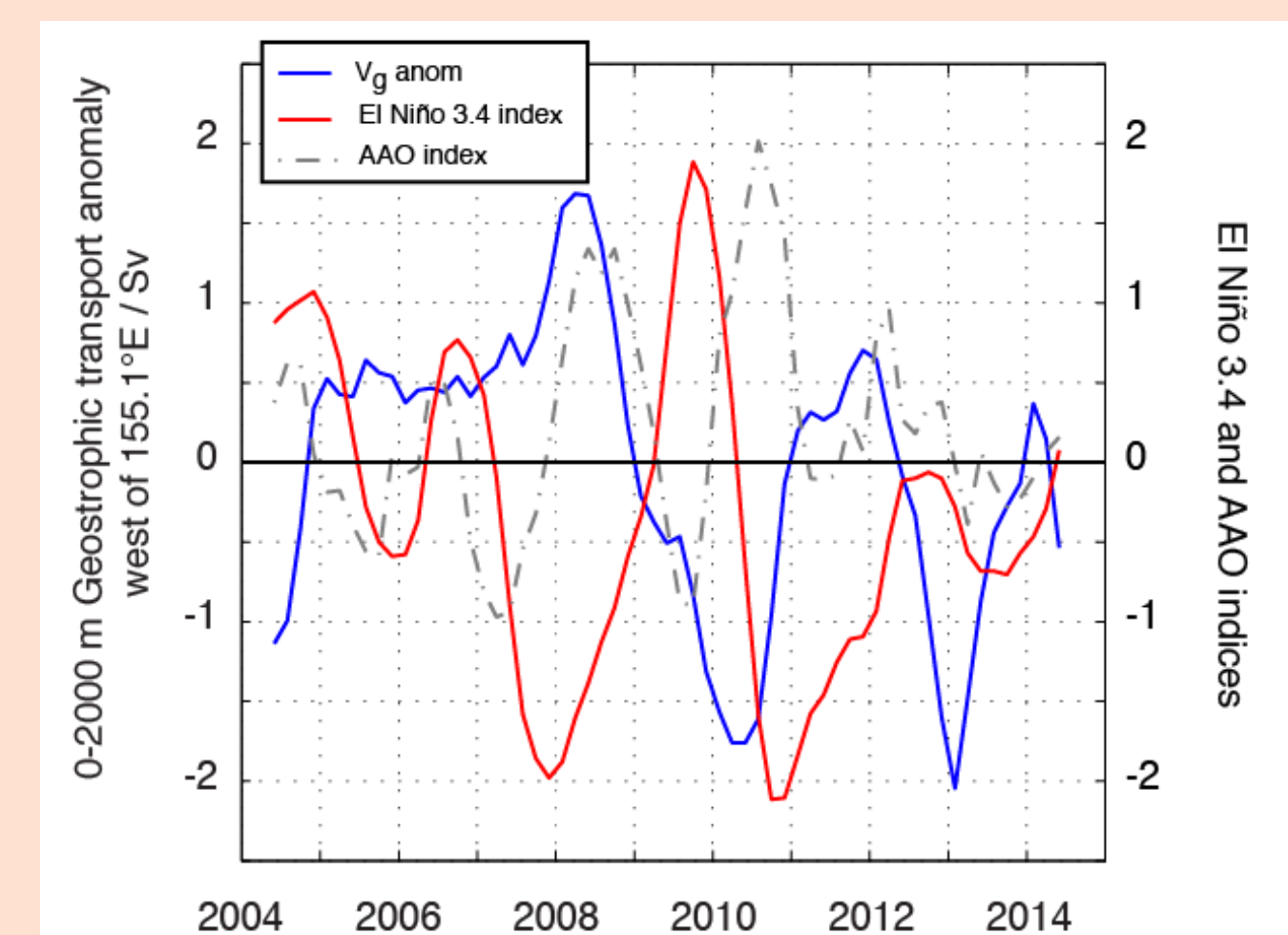


EAC transport west of 155.1°E using XBT/Argo with reference velocity from trajectories is 19.9 Sv (0.4 Sv higher than using a level of no motion at 2000 m), consistent with moored observation by Sloyan et al. (2015).

The XBT/Argo transport estimate agrees within uncertainties with observations from the PCM3 moored array at 30°S by Mata et al. (2000).

Interannual variability of the volume transport in the EAC

The 0-2000 m geostrophic transport west of 155.1°E computed at PX30 with XBT/Argo/altimetry data shows ± 1.0 Sv variability at interannual time scales. The ENSO signature seen in EAC transport anomalies is more evident during strongest El Niño and La Niña events. Argo observations at 32°S show a strong SAM signature in the EAC transport (Zilberman et al., 2014). Our measurements indicate no evident SAM signal at PX30.

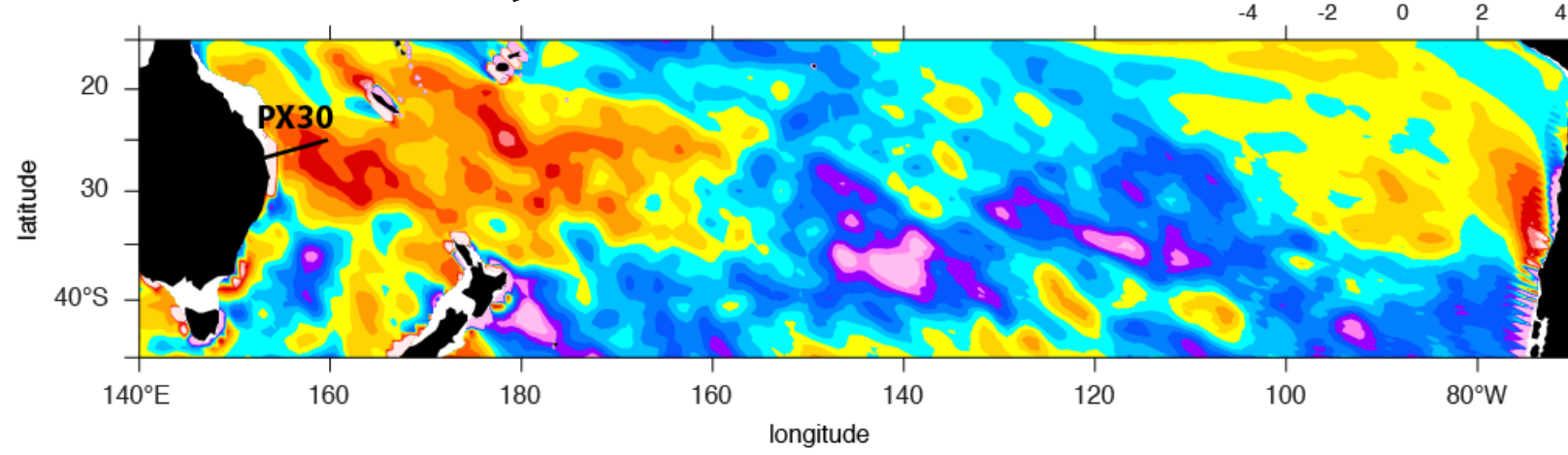


Strong ENSO-related wind-stress curl anomaly at PX30

El Niño: wind-stress curl is more positive, sea level rises in the western Pacific, poleward EAC transport increases.

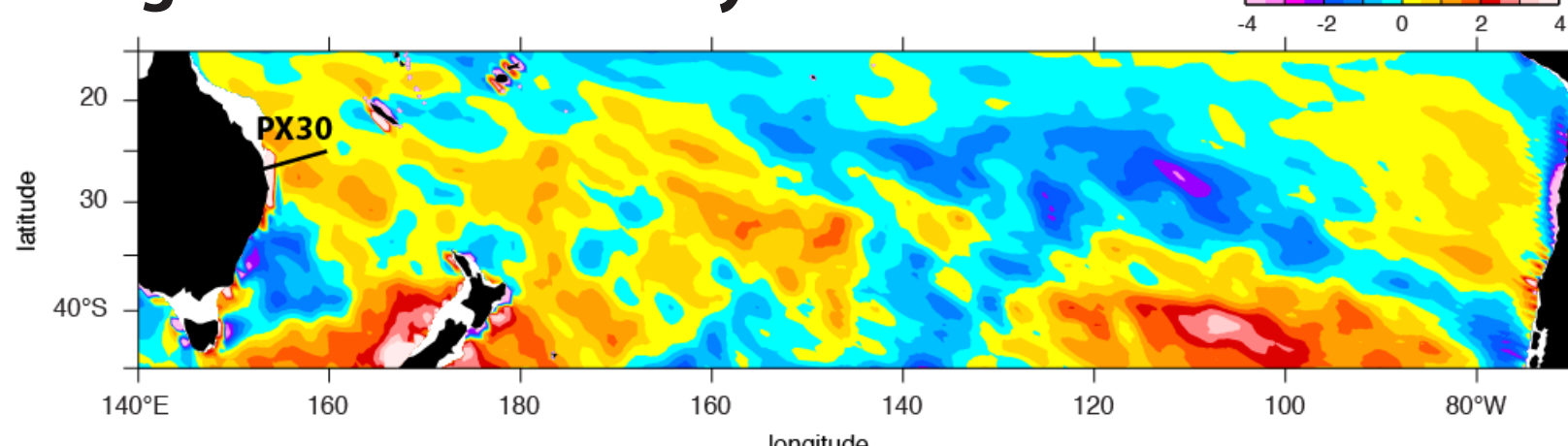
La Niña: wind-stress curl is less positive, sea level decreases in the western Pacific, poleward EAC transport decreases.

El Niño anomaly for 2004-2014



Weak SAM-related wind-stress curl anomaly at PX30 (Strong SAM signal, weak ENSO signature at 32°S)

Negative SAM anomaly for 2004-2014



Summary

The XBT transects, because of their high resolution, are well suited for 0-800 m shear estimates of WBCs. Combining XBT with altimetry provides the needed temporal resolution missing in XBT alone. Argo profiles extend shear estimates to 2000 m. Argo trajectories provide reference velocity to XBT for absolute velocity estimates. A method for combining altimetric data with XBT and Argo profiles to improve the resolution of small scale features and limit sampling errors in the XBT/Argo datasets is developed. XBT/Argo/altimetry based estimates of the geostrophic velocities and transport agree with Sloyan et al. (2015). Geostrophic transport anomalies in the EAC show variability at interannual times scales related to ENSO.

Mata, M. M., M. Tomczak, S. Wijffels, and J. A. Church (2000), East Australian Current volume transports at 30°S: Estimates from the World Ocean Circulation Experiment hydrographic sections PR11/P6 and the PCM3 current meter array, *J. Geophys. Res.*, 105(C12), 28,509–28,526.

Sloyan, B. M., K. R. Ridgway, and R. Cowley, The East Australian Current and Property Transport at 27°S, *J. Phys. Oceanogr.*, submitted.

Zilberman, N. V., D. H. Roemmich, and S. T. Gille, Estimating meridional transport in the East Australian Current, *J. Atmos. Oceanic Technol.*, to be submitted.

Zilberman, N. V., D. H. Roemmich, and S. T. Gille (2014), Meridional volume transport in the South Pacific: Mean and SAM-related variability, *J. Geophys. Res. Oceans*, 119:2658-2678, doi: 10.1002/2013JC009688.

Support from NOAA's Climate Observations Division and from NASA, both for the collection of datasets used here, and for the analysis, is gratefully acknowledged.